

Random-field effects in the diluted two-dimensional Ising antiferromagnet $\text{Rb}_2\text{Co}_{0.7}\text{Mg}_{0.3}\text{F}_4$

R. J. Birgeneau

Department of Physics, Massachusetts Institute of Technology, Cambridge, Massachusetts 02139

H. Yoshizawa, R. A. Cowley,* and G. Shirane
Brookhaven National Laboratory, Upton, New York 11973

H. Ikeda

Department of Physics, Ochanomizu University, Ohtsuka, Bunkyo-ku, Tokyo 112, Japan

(Received 7 March 1983)

We report a comprehensive neutron scattering study of the spin correlations in the diluted two-dimensional (2D) Ising antiferromagnet $\text{Rb}_2\text{Co}_{0.7}\text{Mg}_{0.3}\text{F}_4$ in an applied magnetic field. As predicted by Fishman and Aharony, an applied field in this system produces a random staggered magnetic field. Random fields are expected to have drastic effects on the cooperative behavior of magnets although the detailed behavior remains controversial. It is found that the applied magnetic field, and by inference the concomitant random staggered fields, destroy the 2D long-range order for all temperatures and fields. The structure factor $\mathcal{S}^{\mathbf{z}}(\vec{Q}) = \sum_{\vec{r}} e^{i\vec{Q}\cdot\vec{r}} \langle S_{\vec{r}}^z \cdot S_{\vec{r}+\vec{Q}}^z \rangle_T$ is well described as the sum of a Lorentzian plus a Lorentzian squared with the Lorentzian-squared term dominating at low temperatures. The integrated intensity of the Lorentzian-squared term exhibits the same temperature dependence as the Bragg intensity at zero field. The correlation length κ and structure-factor peak intensity $\mathcal{S}^{\mathbf{z}}(\vec{Q}_0)$ exhibit power-law dependences on the applied field H , $\kappa \sim H^{1.6}$, and $\mathcal{S}^{\mathbf{z}}(\vec{Q}_0) \sim H^{-3.2}$ at low temperatures; the measured exponents agree reasonably with the values 2 and -4 , respectively, deduced from theories with the lower marginal dimensionality $d_l=3$. The effective exponents initially increase slightly with increasing temperature and then decrease dramatically as $T \rightarrow T_N$, taking on values of about 0.7 and -1.2 , respectively, at $T_N=42.5$ K. For small but nonzero applied fields the inverse correlation length may be factorized into a random-field part and a thermal part, $\kappa = \kappa_{\text{RF}} + \kappa_T$, with $\kappa_T \sim e^{-3.4J^{\mathbf{z}}/k_B T}$ where $J^{\mathbf{z}}$ is the Ising exchange constant. It is also found that for $T < 20$ K reproducible results are only obtained when the sample is cooled in the presence of the applied field; this history-dependent behavior is analogous to that found in spin-glasses.

I. INTRODUCTION

In a magnetic system the simplest types of disorder involve randomness in either the interaction strength¹ or the field conjugate to the order parameter.² It is now generally believed that small randomness in the interactions is quite benign. Specifically, if the specific-heat exponent α of the pure system is negative, then there is no change in the critical behavior at all,¹ whereas if α is positive there is a crossover to a new phase transition³ characterized by a negative α . Random fields, however, have much more interesting and dramatic consequences. In a seminal paper, Imry and Ma² suggested that site-random magnetic fields should cause the lower marginal dimensionality d_l to shift from 2 to 4 for continuous symmetry systems and from 1 to 2 for Ising systems. Here d_l is the dimensionality below which the system cannot sustain long-range order (LRO) at finite temperatures. The physical mechanism for the loss of LRO involves a breakup of the system into microdomains in order for it to take advantage of the local random-field energy.

Since Imry and Ma's original work, random-field effects have been the subject of extensive theoretical study. In a series of papers,⁴ culminating in the supersymmetry arguments of Parisi and Sourlas, it has been argued that for dimensionality $d \geq 4$ both Ising and continuous sym-

metry systems with random fields behave like the same system without random fields but in *two fewer dimensions*, that is, $d \rightarrow d-2$. Rigorous extension of this argument to $d < 4$ has proven difficult. The $d \rightarrow d-2$ rule gives $d_l=4$ for continuous symmetry systems in agreement with the simple domain arguments.² However, this concomitantly implies $d_l=3$ for Ising systems in explicit disagreement with smooth domain-wall arguments which predict $d_l=2$. Since the Parisi-Sourlas work, a number of theoretical papers have appeared which address explicitly the issue of d_l for the Ising model in a random field.⁵ Theories based on supersymmetry⁶ all yield $d_l=3$, whereas recent direct calculations of domain-wall energetics⁷ suggest $d_l=2$.

Clearly, therefore, there is an important need for experimental studies of the Ising model in a random field. Such measurements should elucidate not just the d_l issue discussed above but, more generally, the field- and temperature-dependent behavior of such systems. As we shall show, quite interesting and novel effects are indeed observed. It has been known for some time that random fields conjugate to the order parameter occur in a variety of physical systems.⁸ Typically, however, these random fields involve some sort of structural disorder which is not directly controllable. Fishman and Aharony,⁹ however, have made the important observation that a uniform field applied to a random Ising antiferromagnet will generate

random staggered magnetic fields with $\langle H_{\text{RF}}^2 \rangle \sim H^2$ at small magnetic fields. This may easily be seen by noting that in a site-random two-sublattice antiferromagnet the Zeeman term may be written

$$\mathcal{H}_z = \sum_{\langle i,j \rangle} H^z \frac{M_i + M_j}{2} (S_i^z + S_j^z) + \sum_{\langle i,j \rangle} H^z \frac{M_i - M_j}{2} (S_i^z - S_j^z), \quad (1)$$

where i and j represent site variables for the two sublattices. Clearly, if M_i and M_j can take on different values at random, the second term acts like a random staggered field.¹⁰ Fishman and Aharony⁹ actually considered bond randomness which yields an additional term due to the randomness in the exchange field from the induced moment. Clearly these results open up the possibility of systematic studies of the effects of random fields because the field strength can be controlled and varied continuously.

In this paper we report the results of a detailed neutron scattering study of the spin correlations in the site-random *two-dimensional* (2D) Ising antiferromagnet $\text{Rb}_2\text{Co}_{0.7}\text{Mg}_{0.3}\text{F}_4$ in a magnetic field. The magnetic properties of this compound will be discussed extensively below. The experiments show directly the destruction of LRO by the random magnetic field. This result by itself necessitates $d_i \geq 2$, and indeed the correlation-length and structure-factor measurements are consistent with $d_i \approx 3$. Interesting temperature-dependent behavior is observed for which there is, as yet, no theory.

The format of this paper is as follows. In Sec. II A we review the known crystallographic, magnetic, and phase-transition properties of $\text{Rb}_2\text{Co}_{0.7}\text{Mg}_{0.3}\text{F}_4$. In Sec. II B the theory required for the interpretation of the experimental measurements is discussed. The experimental results and analysis are given in Sec. III. Our analysis and interpretation are presented in Sec. IV. Conclusions are given in Sec. V. A preliminary report of the low-temperature measurements has been given in Ref. 11.

II. PRELIMINARY DETAILS

A. $\text{Rb}_2\text{Co}_{0.7}\text{Mg}_{0.3}\text{F}_4$

Rb_2CoF_4 , which has the K_2NiF_4 crystal and magnetic structure,¹² has been shown to constitute a good realization of the 2D square-lattice nearest-neighbor Ising model. The effective Hamiltonian which describes the magnetic behavior of this material is written as¹³

$$\mathcal{H} = \sum_{i,j} [J^z S_i^z S_j^z + J^{\perp} (S_i^x S_j^x + S_i^y S_j^y)] + \sum_i \mu_B \vec{H} \cdot \vec{g} \cdot \vec{S}_i,$$

with $J^z = 7.73 \pm 0.06$ meV, $J^{\perp} = 4.27 \pm 0.17$ meV, $g_{zz} \equiv g_{\parallel} = 7.02 \pm 0.05$, $g_{xx} = g_{yy} \equiv g_{\perp} = 3.07$, and $S = \frac{1}{2}$. The transverse coupling J^{\perp} influences the dynamics but it has no effect on either the order-parameter behavior or the longitudinal instantaneous spin correlations. It should be similarly benign in the random-field disorder regime.

A site-diluted 2D Ising antiferromagnet may be realized simply by replacing the Co^{2+} by Mg^{2+} . Extensive information^{14,15} is now available on the alloy series $\text{Rb}_2\text{Co}_x\text{Mg}_{1-x}\text{F}_4$ including concentrations spanning the percolation threshold $x_p = 0.593$. It is found that

$\text{Rb}_2\text{Co}_{0.59}\text{Mg}_{0.41}\text{F}_4$ indeed exhibits the behavior predicted for the 2D Ising model at percolation.¹⁵

We have chosen the concentration $\text{Rb}_2\text{Co}_{0.7}\text{Mg}_{0.3}\text{F}_4$ for our study of random-field effects for several reasons. Firstly, in order to maximize the relative size of the random fields the concentration of the diluent should be large. At the same time, the system should be far enough from x_p that percolation multicritical effects do not enter. For $x = 0.70$, more than 98% of the Co^{2+} ions belong to the infinite network and the isolated clusters are quite small; this implies that one is well outside of the percolation critical region. Secondly, it has been shown previously¹⁴ that the explicit sample used in these measurements is of quite high quality. The sample orders antiferromagnetically at $T_N = 42.5$ K with a spread in Néel temperatures of about ± 0.5 K, presumably due to a small concentration gradient. The correlation length and staggered susceptibility above T_N exhibit the expected 2D Ising critical behavior. The only significant difference from the pure Ising model is that the bare length is enhanced by about a factor of 4 in the 70% sample. Because of this length enhancement it turns out that the experimental resolution and the smearing of T_N represent equivalent limitations in the zero-field measurements. As we shall show, the smearing of T_N does not have a significant effect on our random-field measurements.

B. Random-field effects and neutron scattering

In order to provide a framework for discussing the experimental results we first consider the possible consequences of random fields on the measured profiles. In a quasielastic neutron scattering experiment in an Ising system the scattering cross section is proportional to the Fourier transform of the two-spin zz correlation function

$$\mathcal{S}^z(\vec{Q}) = \sum_i e^{i\vec{Q} \cdot \vec{r}_i} \langle S_{\vec{r}_i}^z S_{\vec{0}}^z \rangle_T. \quad (2)$$

At high temperatures in zero field, $\mathcal{S}^z(\vec{Q})$ exhibits Lorentzian fluctuations centered about the antiferromagnetic reciprocal-lattice positions \vec{G} , that is,

$$\mathcal{S}^z(\vec{Q}) = \frac{B}{\kappa^2 + q^2}, \quad T > T_N \quad (3)$$

with $\vec{q} = \vec{Q} - \vec{G}$. Since $\text{Rb}_2\text{Co}_{0.7}\text{Mg}_{0.3}\text{F}_4$ has only two-dimensional magnetic correlations, $q^2 = q_x^2 + q_y^2$. For the 2D Ising model¹⁶ $\kappa \sim (T - T_N)$ and $\mathcal{S}^z(\vec{G}) \sim (T - T_N)^{-1.75}$. Below T_N , the cross section in the Ornstein-Zernike approximation is the sum of Lorentzian fluctuation scattering together with the Bragg scattering:

$$\mathcal{S}^z(\vec{Q}) = N \langle S^z \rangle^2 \delta(\vec{Q} - \vec{G}) + \frac{B'}{\kappa^2 + q^2}, \quad T < T_N. \quad (4)$$

Note that B and B' are both proportional to T .

We have already discussed the basic features of the random-field effects in the Introduction. For $d < d_i$ it is believed that the magnetic structure will break up into microdomains²; thus the Bragg term in Eq. (4) must evolve into the structure factor describing the microdomains. On a heuristic basis, one may argue as follows. Lorentzian temperature fluctuations correspond to real-space correlations of the form

$$\langle S_{\vec{r}}^z S_{\vec{0}}^z \rangle_T \sim \frac{e^{-\kappa r}}{r^{(d-1)/2}}. \quad (5)$$

For random-field effects, the supersymmetric theories⁴ suggest that $d \rightarrow d-2$, so that one might expect

$$\langle S_{\vec{r}}^z S_{\vec{0}}^z \rangle_{\text{RF}} \sim \frac{e^{-\kappa r}}{r^{(d-3)/2}}. \quad (6)$$

The Fourier transform of Eq. (6) is just a Lorentzian squared. This then suggests that for $d < d_1$ an appropriate structure factor could be

$$\mathcal{J}^{\text{zz}}(\vec{Q}) = \frac{A}{(\kappa^2 + q^2)^2} + \frac{B}{\kappa^2 + q^2}, \quad (7)$$

where $\vec{q} = \vec{Q} - \vec{G}$. Further we expect $A \sim \langle S^z \rangle_{H=0}^2 \kappa^{4-d}$ for $T < T_N$ and small H_{RF} . The κ^{4-d} normalization is chosen so that the Lorentzian-squared term evolves continuously into the Bragg term in Eq. (4) as H_{RF} , and hence $\kappa \rightarrow 0$. Forms similar to Eq. (7) have been suggested by a number of authors.^{5,17} As noted by Aharony and Pytte,¹⁷ if Eq. (7) is to scale, then $B \sim \kappa^{2-d}$.

For general d , Eq. (7) implies that

$$\mathcal{J}^{\text{zz}}(\vec{G}) \sim \kappa^{-d}, \quad (8)$$

so that one should have $\mathcal{J}^{\text{zz}}(\vec{G}) \sim \kappa^{-2}$ for $\text{Rb}_2\text{Co}_{0.7}\text{Mg}_{0.3}\text{F}_4$. It should be emphasized that Eq. (7) is purely heuristic; it is not at all obvious, for example, that the Lorentzian fluctuations are properly incorporated in Eq. (7). Further, in $d=3$, the scaling requirement $B \sim \kappa^{2-d}$ must be violated. Thus we shall simply use Eq. (7) as a guide with the true form for $\mathcal{J}^{\text{zz}}(\vec{Q})$ to be dictated by experiment.

The theories all predict^{5,6,17} that as $T \rightarrow 0$

$$\kappa \sim H_{\text{RF}}^\nu, \quad (9a)$$

with

$$\nu = \frac{2}{d_1 - d}, \quad d < d_1 \quad (9b)$$

while for $d = d_1$

$$\kappa \sim \exp(-c/H_{\text{RF}}^2). \quad (9c)$$

Clearly, the difference between $d_1=2$ and $d_1=3$ should manifest itself dramatically in these $d=2$ measurements. Finally, using a scaling argument, Aharony and Pytte¹⁷ have predicted that at $T = T_N$ ($H=0$)

$$\nu = \frac{1}{1 - \eta/2} \quad (10a)$$

and

$$\mathcal{J}^{\text{zz}}(\vec{G}) \sim H^{-2}. \quad (10b)$$

Thus with decreasing temperature one would expect a crossover from Eq. (10) to Eq. (9). The explicit form of this crossover has not been predicted theoretically.

III. EXPERIMENTAL RESULTS

A. Experimental configuration and preliminary measurements

The experiments were carried out using a triple-axis spectrometer at the Brookhaven High-Flux Beam Reactor.

As noted in Sec. II A, we used a crystal of $\text{Rb}_2\text{Co}_{0.7}\text{Mg}_{0.3}\text{F}_4$ which had previously been characterized by Ikeda.¹⁴ The sample was approximately $7 \times 10 \times 4 \text{ mm}^3$ in volume. The tetragonal lattice constants at 5 K were $a=4.102 \text{ \AA}$ and $c=13.65 \text{ \AA}$. Some preliminary measurements of the inelastic scattering with and without a magnetic field were made. For these scans the spectrometer was set in a triple-axis configuration with (002) pyrolytic graphite as monochromator and analyzer. The spectrometer was operated either with a fixed incident neutron energy of 50 meV or with a fixed analyzer energy of 24 meV. The crystal was mounted in a cryostat placed in a superconducting magnet. Experiments were carried out with either the [001] or [100] axis vertical so that the field could be applied either parallel or perpendicular to the sublattice moments. Figure 1 shows typical profiles of the scattering from the spin-wave excitations observed at $\vec{Q}=(1-\xi, 2, 0)$ for $\vec{H} \parallel c$ and at $\vec{Q}=(1-\xi, 0, 3.2)$ for $\vec{H} \perp c$. Ikeda and Shirane have previously shown that $\text{Rb}_2\text{Co}_{0.7}\text{Mg}_{0.3}\text{F}_4$ exhibits sharp peaks at 7.0, 14.5, 21.5, and 29.0 meV. Our results are consistent with theirs although the 7.0- and 29.0-meV features are less evident. The four lines correspond to excitation of a single Co ion surrounded by 1, 2, 3, and 4 nearest-neighbor Co ions. We note that 7 meV corresponds to a field of 172 kG. Thus our applied fields of up to 75 kG will always be in the small field region. Spectra with $H=65 \text{ kG}$, both $\vec{H} \parallel c$ and

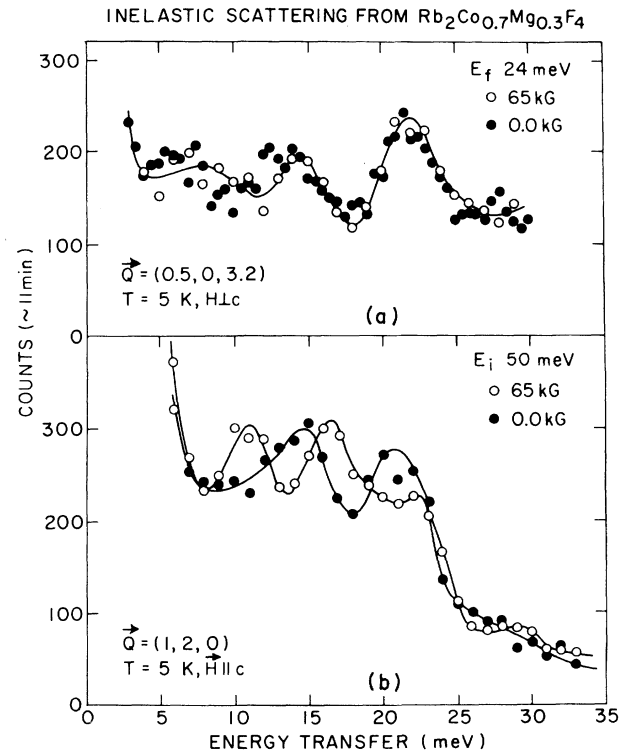


FIG. 1. Inelastic neutron scattering at 5.0 K from $\text{Rb}_2\text{Co}_{0.7}\text{Mg}_{0.3}\text{F}_4$. The upper panel (a) shows the profiles observed at the zone boundary $\vec{Q}=(0.5, 0, 3.2)$ with $H=0 \text{ kG}$ (●) and $H=65 \text{ kG}$ (○) perpendicular to the spin direction, while the lower panel (b) shows the profiles observed at the zone center $\vec{Q}=(1, 2, 0)$ with $H=0$ (○) and $H=65$ (●) kG parallel to the spin direction. The solid lines are guides to the eye.

$\vec{H} \perp c$, are also shown in Fig. 1. The relevant Zeeman energies are, in units of meV,

$$\begin{aligned} g_{\perp} \mu_B H &\sim 1.16, \\ g_{\parallel} \mu_B H &\sim 2.64. \end{aligned} \quad (11)$$

For $\vec{H} \perp c$, the Zeeman energy enters in second order so that no observable effect is expected and indeed none is observed. For $\vec{H} \parallel c$ each peak should split into two with shifts of ± 2.7 meV. The results are qualitatively consistent with these expectations although a detailed calculation of the spin dynamics is required to analyze the field data quantitatively.

The quasielastic scattering experiments were performed in the double-axis configuration with an incident neutron momentum of 2.67 \AA^{-1} . The horizontal collimations were $10'$ throughout and two pyrolytic graphite filters were placed before and after the monochromator to eliminate higher-order contamination in the incident beam. The momentum resolution around $\vec{Q} = [100]_M$ was 0.01 \AA^{-1} full width at half maximum (FWHM) parallel to the scattering vector \vec{Q} and 0.0044 \AA^{-1} FWHM perpendicular to \vec{Q} in the scattering plane. The crystal was mounted with the c axis vertical so that the field was along the spin direction.

As noted above, the phase transition of $\text{Rb}_2\text{Co}_{0.7}\text{Mg}_{0.3}\text{F}_4$ in zero field has previously been studied by Ikeda.¹⁴ We have repeated his measurements and, in general, find complete agreement. For $0.3 > \tau = T/T_N - 1 > 0.025$ one has

$$\kappa\alpha = 0.44(T/T_N - 1)^{1.0}. \quad (12)$$

This is identical to that for the pure 2D Ising model¹⁸ except that the bare length in $\text{Rb}_2\text{Co}_{0.7}\text{Mg}_{0.3}\text{F}_4$ is enhanced by a factor of 4. The phase transition in our crystal is rounded for $\tau < 0.02$. As demonstrated originally by Samuelsen,¹⁹ in these 2D Ising antiferromagnets the degree of correlations between the planes depends on the rate of cooling through the Néel temperature. This effect is enhanced in diluted systems. We find in this crystal at $H = 0$ that if the temperature is lowered in steps of about 1 degree each minute the Bragg scattering takes the form of *rods*, that is, the planes are essentially uncorrelated. We have also verified directly that with a field applied along the c axis the scattering is always purely 2D. Thus in the remainder of this paper the three-dimensional (3D) aspects will be neglected and it will be assumed that the system is ideally 2D.

In order to test the quasielastic approximation for the field-dependent measurements, the quasielastic line shape at $T = 30 \text{ K}$ and $H = 40 \text{ K}$ was compared with that observed in a triple-axis configuration. Within the experimental error both scans gave identical q dependences for the scattering. Further the energy widths at several q values always equalled the instrumental resolution value of 0.1 meV . We conclude, therefore, that the quasielastic approximation is fully satisfied, as one would expect for an Ising system.²⁰

Finally, a limited number of measurements were carried out to study equilibration effects. As we shall discuss extensively in the next subsection, dramatic effects on $\mathcal{I}^z(\vec{Q})$ are indeed observed due to the applied magnetic field. For temperatures greater than 30 K it was explicitly

verified that the spin system equilibrated nearly instantaneously and reproducible results were obtained independent of the direction of approach. On the other hand, at 5 K the spins were "frozen" and did not respond to changes in the applied magnetic field on a time scale of hours. In one set of measurements a field of 45 kG was applied at 5.3 K with no effect. However, on warming to 20 K the observed spectrum was identical to that obtained by cooling from high temperatures in a field of 45 kG . We conclude, therefore, that the crystal reached its true equilibrium state at all fields for $T > 30 \text{ K}$ and certainly for $H \geq 45 \text{ kG}$ at 20 K . All of the experiments reported in the remainder of this paper were obtained by cooling in the field starting from $T > 30 \text{ K}$. The results were then completely reproducible.

B. Field- and temperature-dependent measurements

The principle features of the random-field effects are immediately evident from the qualitative behavior of the quasielastic profiles in the applied magnetic field. Figure 2 shows the temperature dependence of the scattered intensity at the $(100)_M$ antiferromagnetic Bragg position for a series of magnetic fields. It is evident that applied fields very much less than the Co^{2+} molecular fields of about 530 kG have quite drastic effects. The nature of these effects is made clearer by observing the line shapes in the presence of the magnetic field. The field dependence of the profiles observed at $T = 5 \text{ K}$ along the transverse direction $\vec{Q} = (1, \xi, 0)$ is shown in Fig. 3. The upper panel

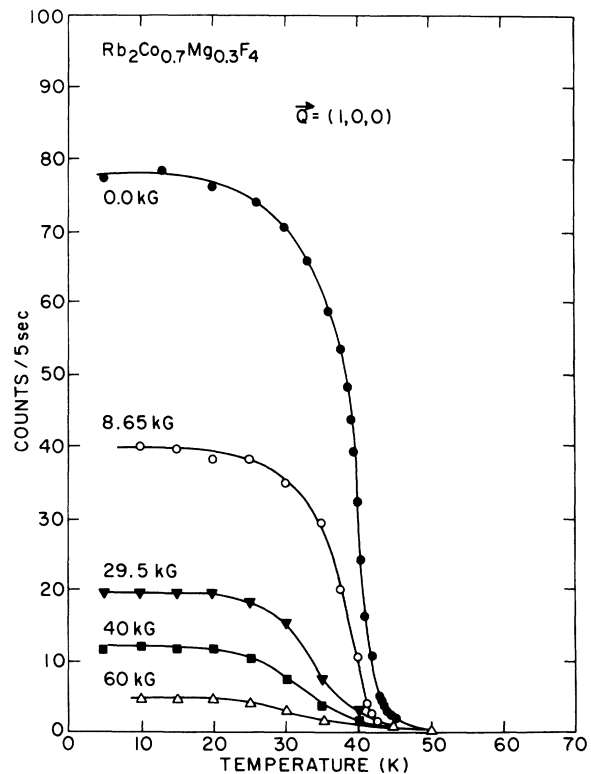


FIG. 2. Peak intensity $\mathcal{I}^z(q=0)$ observed for $\vec{Q} = (1, 0, 0)$ with various magnetic fields $\vec{H} \parallel c$. The solid lines are guides to the eye.

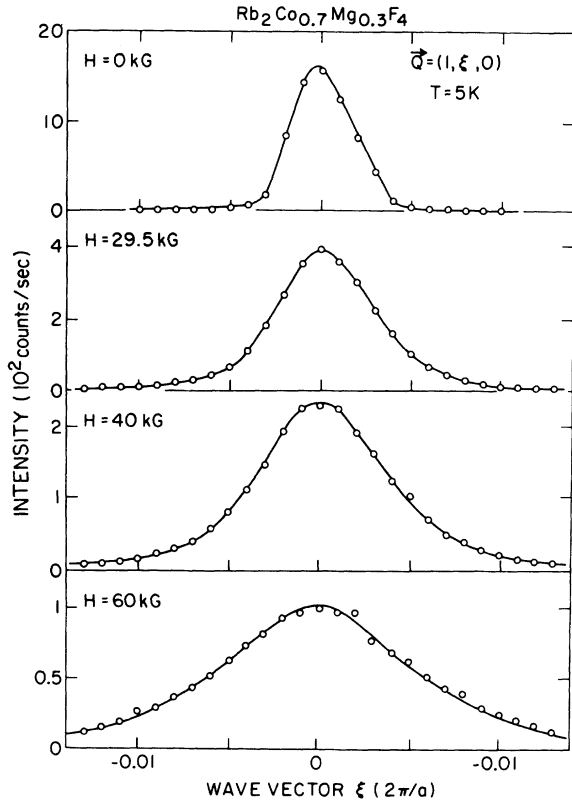


FIG. 3. Quasielastic scattering at 5 K for four different magnetic fields; scans are along the transverse direction $\vec{Q}=(1,\xi,0)$. The solid lines are guides to the eye.

shows the antiferromagnetic Bragg reflection at zero field. This, therefore, simply represents the transverse resolution function of our experiment and is determined by the convolution of the crystal mosaic with the spectrometer resolution function. As noted above, the transverse FWHM is 0.004 reciprocal-lattice units (r.l.u.). When the magnetic field is applied the peak both broadens and exhibits a distinct change in line shape. The width clearly increases rapidly with increasing applied field. Since the reciprocal of the intrinsic FWHM is proportional to the correlation length of the magnetic ordering, the broadening width evident in Fig. 3 shows that the antiferromagnetic long-range order in $\text{Rb}_2\text{Co}_{0.7}\text{Mg}_{0.3}\text{F}_4$ has been destroyed by the applied field. In a pure system magnetic fields much less than the exchange field merely shift the Néel temperature with $\Delta T_N/T_N \sim (H/H_c)^2$. We are confident, therefore, that the destruction of long-range order originates in the random staggered magnetic field generated by the applied magnetic field in this system.

As an additional test of this mechanism we have carried out some limited measurements with the field perpendicular to the c axis. Because of the high symmetry of the Rb_2CoF_4 structure, this will only generate, to leading order, *transverse* random staggered fields. We find in this case that for fields of 65 kG, there is a sharp phase transition to a state with long-range order. Thus, as expected, only random fields conjugate to the order parameter can destroy the long-range order.

Figure 4 shows the temperature dependence of the $(1,\xi,0)$ transverse scans for a field of 40 kG applied along

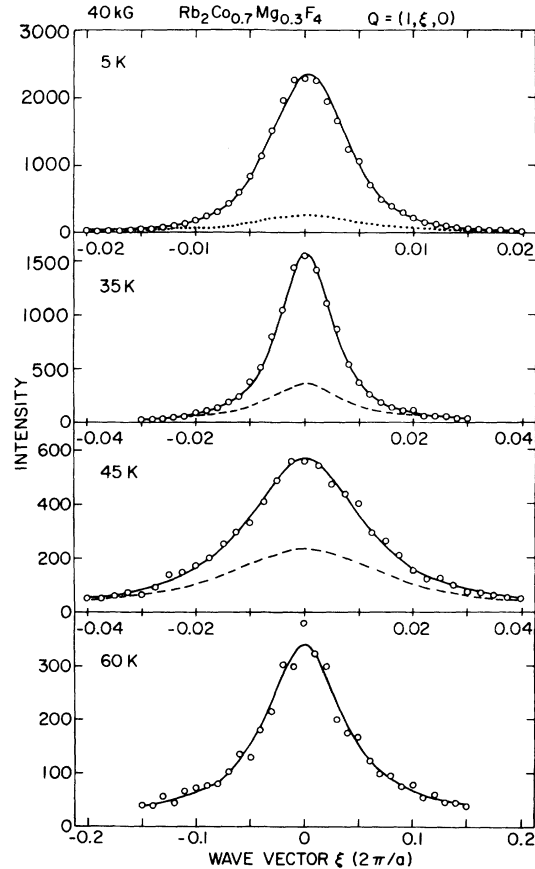


FIG. 4. Quasielastic scattering for 40 kG at four different temperatures. Note that the horizontal and vertical axes change progressively in scales. The solid lines are the best fits of Eq. (7), while the dashed lines indicate the contribution of the Lorentzian term. At 60 K the scattering is purely Lorentzian.

the c axis. Note that the vertical and horizontal scales are adjusted for each panel in order to keep the widths and heights comparable. It is evident that the width decreases progressively with decreasing temperature. It is also clear qualitatively that there is a distinct change in line shape between 60 and 5 K; the scan at 60 K is Lorentzian in character whereas the wings drop off much more rapidly than q^{-2} at 5 K. This was a striking result when it was first observed. From the theoretical discussion given in Sec. II it is evident that just such an effect should be observed as one crosses over from fluctuations dominated by temperature to behavior dominated by the random field. This effect has also been observed in $^{21}\text{Co}_{1-x}\text{Zn}_x\text{F}_2$.

In order to determine the wave-vector dependence of $\mathcal{S}^{\text{zi}}(\vec{Q})$ more accurately, a series of longitudinal scans with quite high statistics were carried out. In this case longitudinal scans along $\vec{Q}=(1+\xi,0,0)$ were employed because the transverse wings were distorted by small mosaic crystallites in our sample. Examples of such scans are shown on a semilogarithmic scale in Figs. 5 and 6. These were measured with the magnetic field fixed at 60 kG and $T=5.3$ and 50 K, respectively. The background was constant at the indicated level throughout the relevant wave-vector region. A detailed analysis of the wave-vector

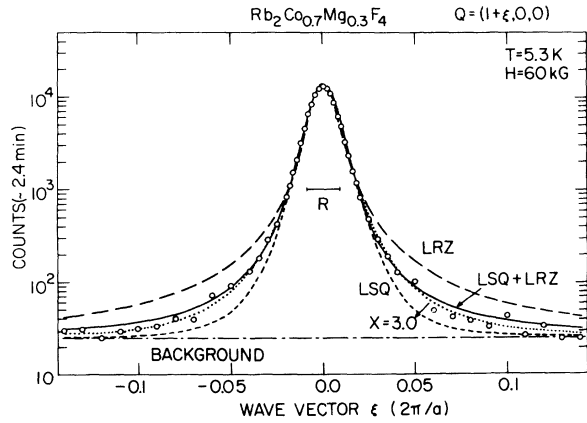


FIG. 5. Quasielastic scattering observed along the longitudinal directional direction $\vec{Q}=(1+\xi,0,0)$ at 5.3 K with $H=60$ kG. The best fits to the Lorentzian (a long-dashed line), to the Lorentzian squared (a short-dashed line), to Eq. (7) (a solid line), and to Eq. (13) (a dotted line) are shown. R indicates the instrumental resolution.

dependence of these profiles will be presented in the next section.

From a series of scans including those shown in Figs. 3 and 4, the transverse FWHM could be determined as a function of temperature for various fields. These data are summarized on a semilogarithmic scale in Fig. 7. Here the width of the antiferromagnetic Bragg reflection, which represents the transverse resolution, is shown by a dashed line. For all fields there is a crossover from a high-temperature region dominated by thermal fluctuations to a low-temperature region dominated by random-field fluctuations. We remind the reader that these data represent the true equilibrium state for all H for $T \geq 30$ K and for $T \geq 20$ K provided $H \geq 45$ K. This does not mean that all other data correspond to nonequilibrium states but rather that we did not test for equilibration at smaller fields for temperatures in the neighborhood of 20 K. At 5 K the

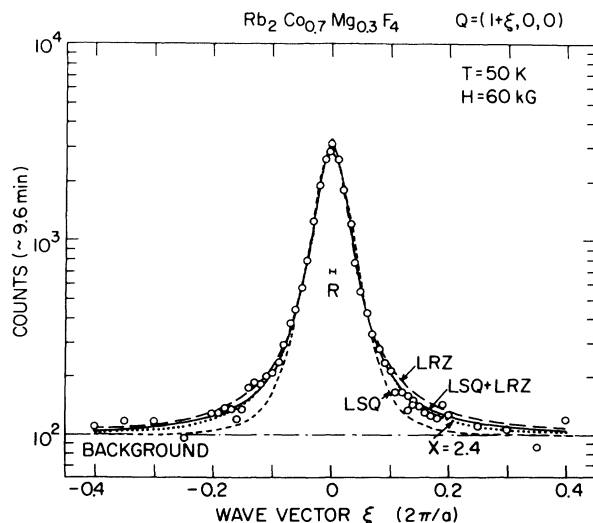


FIG. 6. Quasielastic scattering observed along the longitudinal directional $\vec{Q}=(1+\xi,0,0)$ at 50 K with $H=60$ kG. The best fits to various analytic forms are also shown.

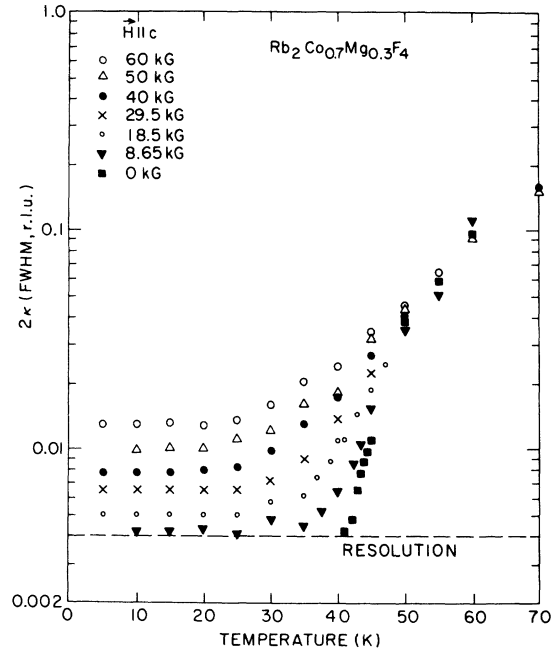


FIG. 7. Temperature dependence of the full width at half maximum of the quasielastic scattering of $\text{Rb}_2\text{Co}_{0.7}\text{Mg}_{0.3}\text{F}_4$ with various magnetic fields.

system certainly is frozen for the range of fields employed in these experiments. We note also that reproducible results were obtained at all temperatures provided that one cooled the sample in the magnetic field.

It is evident from the FWHM data in Fig. 7 that there is no indication of a phase transition at nonzero applied fields. In order to probe this further, the critical scattering just off the Bragg peak at $(-0.008,1,0)$ was monitored as a function of temperature. In a normal phase transition the critical scattering exhibits a sharp peak at T_N as $\vec{Q} \rightarrow \vec{G}$. In this sample with $H=0$, the peak is somewhat broadened due to the concentration gradient. Nevertheless, with the application of a magnetic field one could clearly observe both a shift in the critical scattering peak temperature and a progressive broadening with increasing field. We observe shifts in the peak temperature of 0.2, 1.0, 1.6, and 4.0 K at fields of 4.5, 8.65, 14.0, and 20 kG, respectively. By comparison with Fig. 7 these peak temperatures appear to occur in the middle of the transition region from temperature-dominated to random-field-dominated behavior. We might note that $\Delta T \sim H^{1.7}$ although the exponent is only known roughly. This appears to be somewhat more rapid than the behavior $\Delta T_N \sim H^{2/\gamma} = H^{1.2}$, which would obtain for the shift in Néel temperature predicted for a random-field system above its lower marginal dimensionality.¹⁰

In order to discuss these data quantitatively it is necessary to carry out a detailed line-shape analysis. Accordingly, we now present the results of our fits to the data.

IV. ANALYSIS AND DISCUSSION

It has been noted in the preceding section that at high temperatures the profiles are Lorentzian whereas at lower temperatures in the applied field the wings fall off more rapidly than q^{-2} . Indeed double-logarithmic plots of the

tail intensities against reduced wave vector give slopes in the neighborhood of 3 at low temperatures. It is clear that Eq. (7), which has terms exhibiting q^{-4} and q^{-2} dependences, could simulate such behavior. Equivalently one could try a structure factor of the form

$$\mathcal{I}^{\text{zz}}(\vec{Q}) = \frac{C}{(\kappa^2 + q^2)^{x/2}}, \quad (13)$$

where again $\vec{q} = \vec{Q} - \vec{G}$.

The results of fits to Eqs. (7) and (13) are illustrated in Figs. 5 and 6 for $H = 60$ kG. In the quasicrystalline phase at 5.3 K (Fig. 5) fits to a single Lorentzian (LRZ) give systematic deviations over the complete range of wave vectors. The Lorentzian-squared form (LSQ) fits the central region down to the 5% level in intensity quite well. However, the distant tails drop off less rapidly than the q^{-4} behavior of a pure LSQ. Not surprisingly then, fits to Eq. (7), which is the sum of a LRZ and a LSQ, work quite well over the complete wave-vector range. As illustrated in Fig. 5, Eq. (13) with $x = 3.0$ works equally well, and from the data we cannot determine whether Eq. (7) or (13) is correct. As shown in Fig. 6, at $T = 50$ K the data are reasonably well described by a pure LRZ. The quality of the fit is improved slightly by including a small LSQ term. The profiles are also well described by Eq. (13) with $x = 2.4$. We have analyzed all of the data using both Eq. (7) and Eq. (13) for $\mathcal{I}^{\text{zz}}(\vec{Q})$. The consequent temperature and field dependences of κ and $\mathcal{I}^{\text{zz}}(\vec{G})$ are closely similar for both forms so that conclusions drawn from one also hold for the other. Since Eq. (7) is preferred by current theory we shall focus our discussion primarily on the results obtained explicitly from fits to the LSQ + LRZ form, Eq. (7).

The results of these fits to the data are summarized in Figs. 8–10. We discuss first the results at low temperatures. The fitted parameters are essentially independent of temperature for $T \leq 20$ K. To within the errors it is found that at low temperatures

$$\mathcal{I}^{\text{zz}}(\vec{G}) \sim \kappa^2. \quad (14)$$

This confirms the prediction, Eq. (8), which we made using continuity arguments and Aharony and Pytte¹⁷ derived using scaling arguments. It is found, in addition, that the Lorentzian amplitude B , shown in the lower panel of Fig. 10, is only weakly dependent on field. This is also consistent with the scaling prediction $B \sim \kappa^{2-d}$.

The behavior of K and $\mathcal{I}^{\text{zz}}(\vec{G})$ as a function of field is shown in Fig. 11. It is evident that both exhibit power-law dependences on H ,

$$\begin{aligned} \kappa &\sim H^{1.6 \pm 0.1}, \\ \mathcal{I}^{\text{zz}}(\vec{G}) &\sim H^{-3.2 \pm 0.2}, \end{aligned} \quad (15)$$

at low temperatures.

The destruction of the long-range order by the random field demonstrates explicitly that $d_l \geq 2$. As noted in Sec. II all current theories predict exponential behavior in H_{RF}^{-2} at d_l , Eq. (9c), and power-law behavior for $d < d_l$. It is clear from Fig. 11 that power-law rather than exponential behavior obtains in $\text{Rb}_2\text{Co}_{1-x}\text{Mg}_x\text{F}_4$ at low temperatures. From Eqs. (8) and (9b) one has for $d_l = 3$, $\kappa \sim H_{\text{RF}}^{-2}$ and $\mathcal{I}^{\text{zz}}(\vec{G}) \sim H_{\text{RF}}^{-4}$. This is in qualitative agreement with our

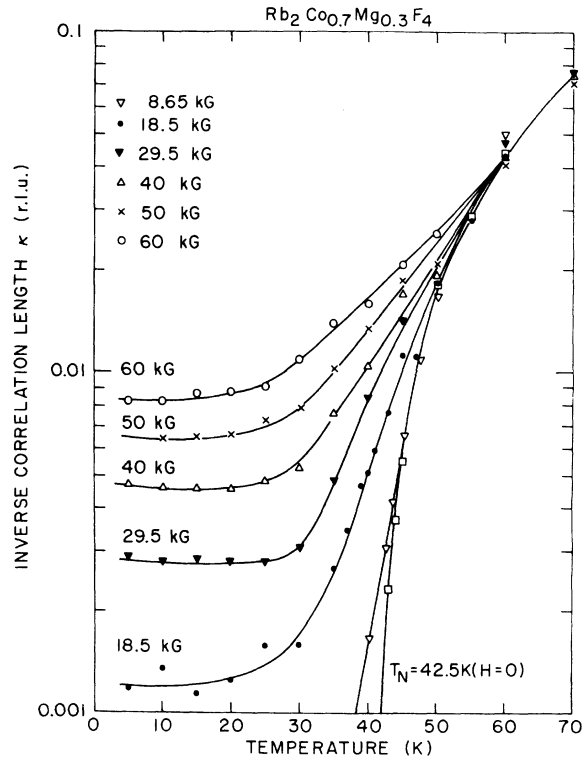


FIG. 8. Resolution-corrected inverse correlation length K in $\text{Rb}_2\text{Co}_{0.7}\text{Mg}_{0.3}\text{F}_4$ at various fields as a function of temperature. The solid lines are guides to the eye. The units are $2\pi/a_M = 1.083 \text{ \AA}^{-1}$.

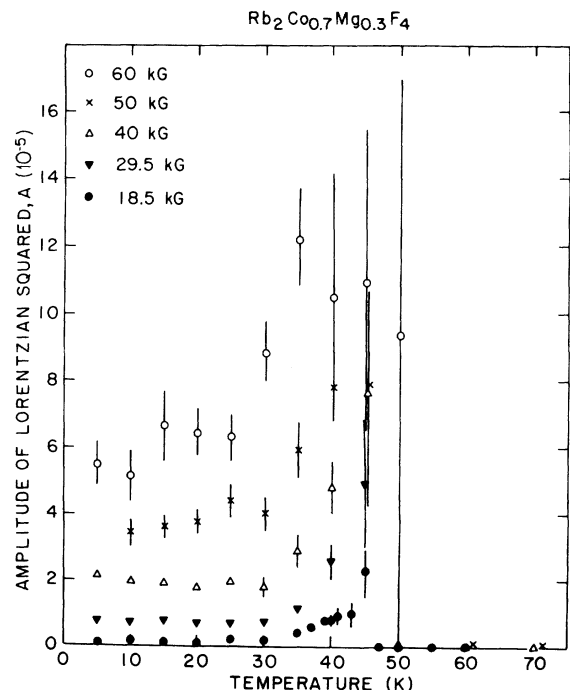


FIG. 9. Temperature dependence of the amplitude A of the Lorentzian-squared term in Eq. (7) for five different magnetic fields.

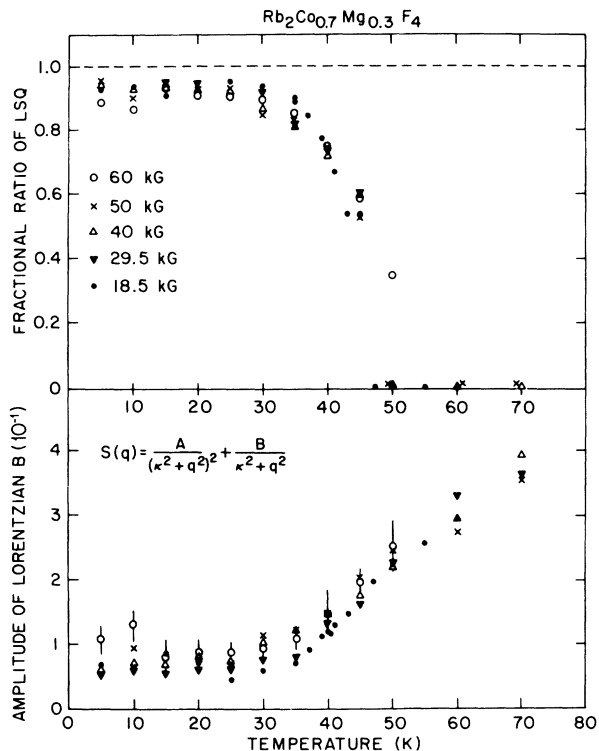


FIG. 10. Upper panel shows the fractional contribution of the Lorentzian-squared term to the total intensity at the peak position. The lower panel shows the temperature dependence of the amplitude of the Lorentzian B for the five different magnetic fields.

results, Eq. (15). There are a number of possible reasons for the slight discrepancy in the exponents including higher-order terms in either H_{RF} vs H or in the theoretical predictions, Eqs. (8) and (9), themselves.

Before discussing the d_l issue further, we consider the evolution of κ vs H with temperature. We show in Fig. 12, κ vs H for $T = T_N = 42.5$ K and for $T = 40, 35, 30, 20$, and 10 K. Note that 20 and 10 K yield identical results. The data at the higher temperatures are, unfortunately, somewhat sparse. Nevertheless, the trend is quite clear. At T_N the data are consistent with $\kappa_{T_N} \sim H^{0.7 \pm 0.2}$. This may be compared with the Aharony-Pytte¹⁷ scaling prediction

$$\kappa_{T_N} \sim H^{(1-\eta/2)^{-1}} = H^{1.14}.$$

The measured exponent again is somewhat smaller than the theoretical value but, given the sparseness of the data, we do not regard this discrepancy as serious. A more accurate test of Eq. (10) will require a crystal with a much smaller concentration gradient. As the temperature is lowered below T_N , the logarithmic slope (Fig. 12) increases gradually, reaching a maximum at 30 K, where κ (30 K) $\sim H^{1.7 \pm 0.1}$, and decreases slightly with decreasing temperature. It should be recalled that at 30 K for all fields the true equilibrium state is attained whereas at 20 K only the $H > 45$ kG points were explicitly demonstrated to be in equilibrium; the points at 20 K with $H = 18.5, 29.5$, and 40 kG fall on a smooth extrapolation of the high-field data so that they too probably represent the true

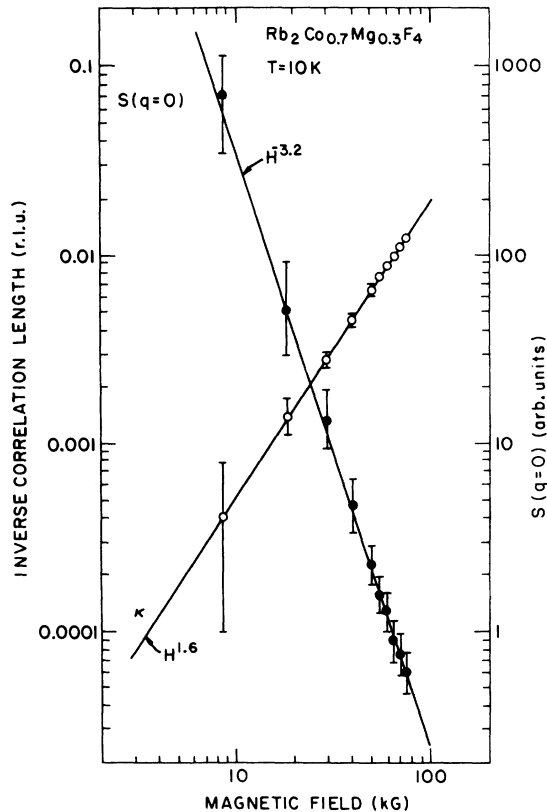


FIG. 11. Dependences of the inverse correlation length and the peak intensity of the quasielastic scattering from $\text{Rb}_2\text{Co}_{0.7}\text{Mg}_{0.3}\text{F}_4$ on the applied magnetic field at 10 K.

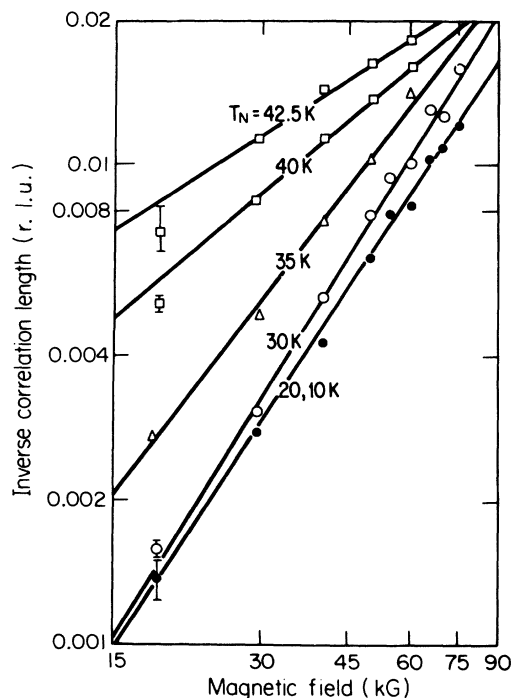


FIG. 12. Logarithmic plot of the fitted inverse correlation length κ vs magnetic field at a series of temperatures. Data at 20 and 10 K are indistinguishable.

equilibrium state. There is, at present, no theory for the evolution of κ vs H from high to low temperatures. It is clear, nevertheless, that the data evolve smoothly with decreasing temperature and it appears that Eq. (15) represents the correct low-temperature behavior. Certainly there is no evidence of a crossover to the exponential form, Eq. (9c). We regard this as strong evidence that $d_l > 2$ and is probably close to 3. Indeed, interpreted literally using Eq. (9b), the data would imply $d_l = 3.2$. Similar experiments²¹ in $\text{Co}_x\text{Zn}_{1-x}\text{F}_2$, if similarly directly interpreted, suggest that $d_l > 3$.

An additional prediction of our heuristic theoretical arguments presented in Sec. II was that at small fields the integrated intensity of the Lorentzian-squared component of the total scattering should scale as the order parameter squared. Accordingly, we plot A/κ^2 from Figs. 8 and 9 for $H = 18.5$ and 29.5 kG; we have normalized the mean of all data for $T \leq 20$ K to unity. The results are plotted in Fig. 13 together with the measured Bragg intensity. Clearly the agreement is very good. There is some rounding near T_N as one would expect since the data are far from the $H \rightarrow 0$ limit. As discussed by Hagen *et al.*,²¹ similar agreement is found in the 3D Ising system $\text{Co}_{1-x}\text{Zn}_x\text{F}_2$. This behavior is illustrated in an alternate form by plotting the fractional ratio of the LSQ term to the total scattering at $q = 0$; this is shown in the top panel of Fig. 10.

One of the important issues in the theoretical description of the random-field problem is the correct choice of temperature variables. Some information about this problem may be obtained empirically from the temperature dependence of κ . For $\text{Rb}_2\text{Co}_{1-x}\text{Mg}_x\text{F}_4$ at the percolation threshold, the inverse correlation length may be written¹⁵

$$\kappa(x, T) = \kappa(x, 0) + \kappa(0, T), \quad (16)$$

that is, the thermal and geometrical inverse correlation

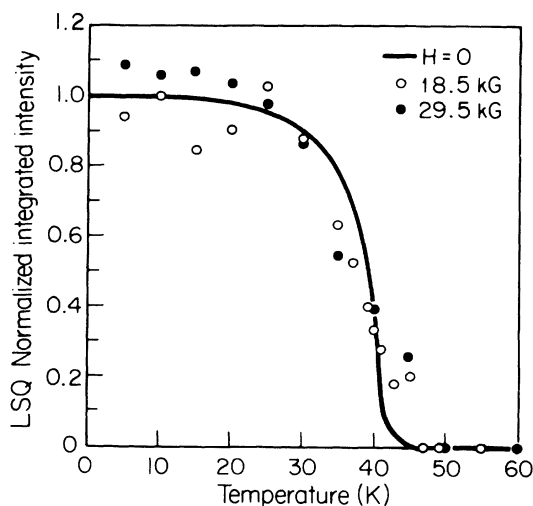


FIG. 13. Normalized integrated intensity of the Lorentzian-squared part of the scattering at 18.5 and 29.5 kG. The solid line is the measured Bragg scattering at $H = 0$ normalized to unity at 5 K.

lengths simply add. Further, one finds¹⁵

$$\kappa(Q, T) \sim \exp \left[- \left(\frac{J^z}{k_B T} \right)^{\nu_T} \right], \quad (17)$$

where $\nu_T = 1.33$ is the appropriate percolation critical exponent. It is tempting to analyze the random-field data using a form analogous to Eq. (16), that is,

$$\kappa(H, T) = \kappa(H, 0) + \kappa(0, T). \quad (18)$$

We show in Fig. 14 the values for $\kappa_{\text{th}} \equiv \kappa(0, T)$ obtained in this fashion plotted in semilogarithmic form against $1/T$. The results are clearly very suggestive. For fields up to 40 kG the factorization Eq. (18) is quite good. Further, κ_{th} is well represented by the form

$$\kappa_{\text{th}}(\text{r.l.u.}) = 3e^{-270/T}. \quad (19)$$

The activation energy, $270k_B$, is remarkably close to the mean molecular-field energy of $\sim 240k_B$ required to flip a single Co^{2+} spin at low temperatures in $\text{Rb}_2\text{Co}_{0.7}\text{Mg}_{0.3}\text{F}_4$. This suggests that for $d < d_l$ thermal effects enter the random-field problem in the simplest fashion possible. Extra complexities due to such effects as the thermal roughening of the interfaces do not seem to be important. These results should provide an important guide for any finite temperature theory of the random-field problem. It should be emphasized that Eqs. (18) and (19) cannot hold all the way to $H = 0$ since one must cross over continuously to the 2D Ising behavior $\kappa \sim (T - T_N)^{1.0}$ as $H \rightarrow 0$.

Finally, for completeness, we show in Fig. 15 the values of the exponent x obtained by fits of the data to the alternative form of the cross section, Eq. (13). As expected, x is about 3 at low temperatures decreasing to 2 for $T > T_N$. As noted previously, the field and temperature depen-

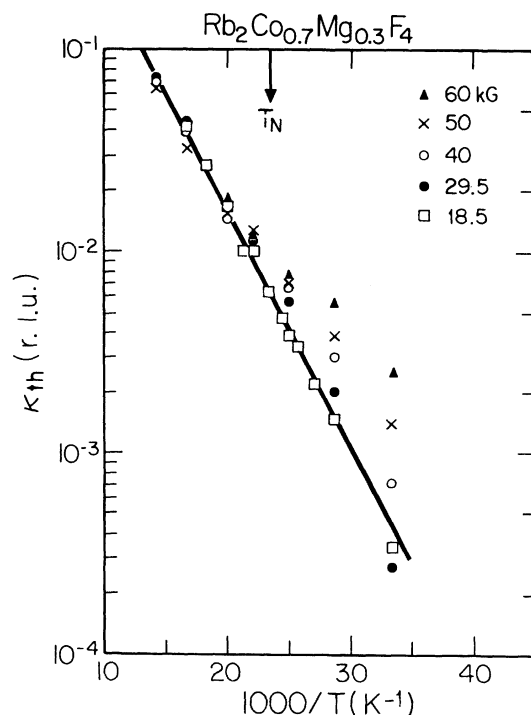


FIG. 14. Semilogarithmic plot of the thermal part of the inverse correlation length of $\text{Rb}_2\text{Co}_{0.7}\text{Mg}_{0.3}\text{F}_4$ against $1/T$.

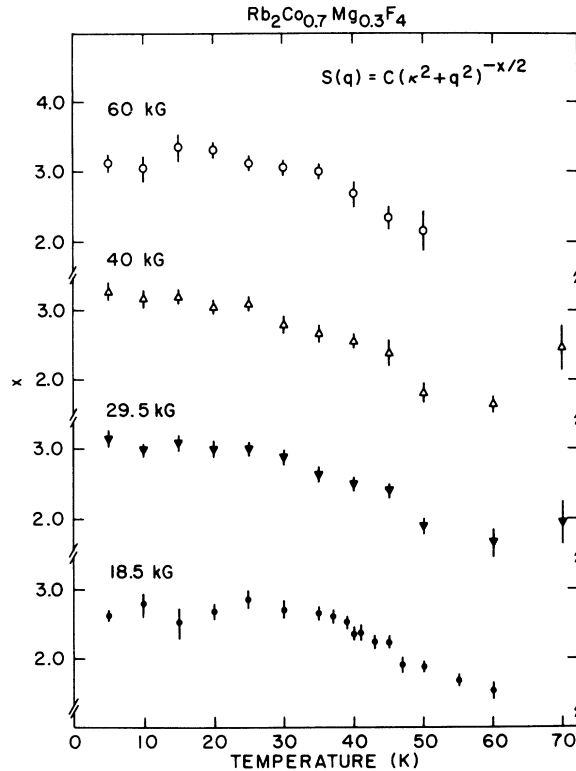


FIG. 15. Temperature dependence of the exponent x defined by Eq. (13).

dences of κ and $\mathcal{S}^z(\vec{G})$ are similar to those deduced using the LRZ + LSQ form, Eq. (7).

V. SUMMARY AND CONCLUSIONS

These experiments have demonstrated that using the suggestion of Fishman and Aharony it is possible to study random-field effects in Ising systems systematically as a function of field and temperature. The experiments show that in the presence of an applied field the diluted 2D antiferromagnet $\text{Rb}_2\text{Co}_{0.7}\text{Mg}_{0.3}\text{F}_4$ evolves continuously from normal temperature-fluctuation behavior at high temperatures to a random-field microdomain state at low temperatures. The low-temperature state is characterized by a novel structure factor which is predominantly Lorentzian squared in character. The amplitude of the Lorentzian-squared term scales as $\kappa^2 \langle S_z \rangle^2 H = 0$, as predicted by

heuristic arguments. At low temperatures we find $\kappa \sim H^{1.6}$, $\mathcal{S}^z(\vec{G}) \sim H^{-3.2}$, which is roughly consistent with the predictions of the $d_l = 3$ theories. Further evidence for $d_l \geq 3$ is found in experiments on the 3D Ising systems $\text{Co}_{1-x}\text{Zn}_x\text{F}_2$.²¹

It is found that for small but nonvanishing fields one may write $\kappa = \kappa(H, 0) + 3e^{-270/T}$ (r.l.u.). This suggests that the relevant temperature scaling field is simply the Boltzmann factor for flipping a Co^{2+} spin in the molecular field due to its neighbors. More exotic effects due, for example, to domain-wall roughening do not seem to be important. It is clear that there is a strong need for theories which treat properly the crossover from the temperature to the random-field dominated regime.

In our view, the only serious caveat in the above is the low-temperature equilibration problems which we have discovered. We have argued that these cannot vitiate our principal conclusion that $d_l > 2$. Nevertheless, it is clearly important to study these effects in systems which equilibrate in reasonable time scales at low temperatures. This may be achievable by studying diluted 2D systems with smaller Ising anisotropies. It should also be emphasized that all of the theory carried out so far is, in fact, for a uniform ferromagnet in the presence of a random field. It is possible that the presence of vacancies will alter the behavior, that is, d_l may be different for the random-field problem with and without vacancies. Only further experiments and theory can clarify this issue. Finally other experiments such as heat capacity and NMR would be valuable in helping us complete our empirical picture of random-field effects in two dimensions.

ACKNOWLEDGEMENTS

We would like to thank A. Aharony, A. N. Berker, K. De'Bell, P. M. Horn, Y. Imry, D. Mukamel, E. Pytte, G. Grinstein, D. J. Wallace, S. M. Shapiro, and G. Aeppli for valuable discussions of this work. The work at Massachusetts Institute of Technology was supported by the National Science Foundation—Low Temperature Physics Program, under Contract No. DMR-79-23203, the work at Brookhaven National Laboratory was supported by the Division of Basic Energy Sciences, U.S. Department of Energy under Contract No. DE-AC02-76CH0016, and that at the University of Edinburgh was supported by the United Kingdom Science Research Council.

*Permanent address: Department of Physics, University of Edinburgh, Mayfield Road, Edinburgh EH9 3JZ, Scotland.

¹A. B. Harris, *J. Phys. C* **7**, 1671 (1974); G. Grinstein and A. Luther, *Phys. Rev. B* **13**, 1329 (1976).

²Y. Imry and S.-k. Ma, *Phys. Rev. Lett.* **35**, 1399 (1975).

³D. E. Khmel'netskii, *Zh. Eksp. Teor. Fiz.* **68**, 1960 (1975) [*Sov. Phys.—JETP* **41**, 981 (1975)]. For recent experiments see R. J. Birgeneau, R. A. Cowley, G. Shirane, H. Yoshizawa, D. P. Belanger, A. R. King, and V. Jaccarino *Phys. Rev. B* **27**, 6747 (1983).

⁴A. Aharony, Y. Imry, and S.-k. Ma, *Phys. Rev. Lett.* **37**, 1367 (1976); G. Grinstein, *ibid.* **37**, 944 (1976); A. P. Young, *J. Phys. C* **10**, L257 (1977); G. Parisi and N. Sourlas, *Phys. Rev.*

Lett. **43**, 744 (1979).

⁵E. Pytte, Y. Imry, and D. Mukamel, *Phys. Rev. Lett.* **46**, 1173 (1981); K. Binder, Y. Imry, and E. Pytte, *Phys. Rev. B* **24**, 6736 (1981); D. Mukamel and E. Pytte, *ibid.* **25**, 4779 (1982).

⁶H. S. Kogon and D. J. Wallace, *J. Phys. A* **14**, L527 (1981); J. Cardy (unpublished); A. Niemi, *Phys. Rev. Lett.* **49**, 1808 (1982).

⁷G. Grinstein and S.-k. Ma, *Phys. Rev. Lett.* **49**, 685 (1982); J. Villain, *J. Phys. (Paris)* **43**, L551 (1982).

⁸See, for example, D. E. Moncton, F. J. DiSalvo, J. D. Axe, L. J. Sham, and B. R. Patton, *Phys. Rev. B* **14**, 3432 (1976); P. Z. Wong, P. M. Horn, R. J. Birgeneau, C. R. Safinya, and G. Shirane, *Phys. Rev. Lett.* **45**, 1974 (1980); G. Aeppli, S. M.

- Shapiro, R. J. Birgeneau, and H. S. Chen, *Phys. Rev. Lett.* **B** 25, 4882 (1982).
- ⁹S. Fishman and A. Aharony, *J. Phys. C* 12, L729 (1979).
- ¹⁰P. Z. Wong, S. von Molnar, and P. Dimon, *J. Appl. Phys.* 53, 7954 (1982).
- ¹¹H. Yoshizawa, R. A. Cowley, G. Shirane, R. J. Birgeneau, H. J. Guggenheim, and H. Ikeda, *Phys. Rev. Lett.* 48, 438 (1982).
- ¹²E. Legrand and R. Plumier, *Phys. Status Solidi* 2, 317 (1962); R. J. Birgeneau, H. J. Guggenheim, and G. Shirane, *Phys. Rev. Lett.* 22, 720 (1979).
- ¹³H. Ikeda and M. T. Hutchings, *J. Phys. C* 11, L529 (1978).
- ¹⁴H. Ikeda, *J. Phys. Soc. Jpn.* 50, 3215 (1981), and references therein.
- ¹⁵R. A. Cowley, R. J. Birgeneau, G. Shirane, H. J. Guggenheim, and H. Ikeda, *Phys. Rev. B* 21, 4038 (1980).
- ¹⁶L. Onsager, *Phys. Rev.* 65, 117 (1944); B. Kaufman and L. Onsager, *ibid.* 76, 1244 (1949).
- ¹⁷A. Aharony and E. Pytte, *Phys. Rev. B* 27, 5872 (1983).
- ¹⁸H. Ikeda and G. Shirane, *J. Phys. Soc. Jpn.* 46, 30 (1979).
- ¹⁹E. Samuelsen, *Phys. Rev. Lett.* 31, 936 (1973).
- ²⁰M. T. Hutchings, H. Ikeda, and E. Janke, *Phys. Rev. Lett.* 49, 386 (1982).
- ²¹M. Hagen, R. A. Cowley, S. Satija, H. Yoshizawa, G. Shirane, R. J. Birgeneau, and H. J. Guggenheim, *Phys. Rev. B* (in press).